
This copy is for your personal, non-commercial use only.

If you wish to distribute this article to others, you can order high-quality copies for your colleagues, clients, or customers by [clicking here](#).

Permission to republish or repurpose articles or portions of articles can be obtained by following the guidelines [here](#).

The following resources related to this article are available online at www.sciencemag.org (this information is current as of January 14, 2011):

Updated information and services, including high-resolution figures, can be found in the online version of this article at:

<http://www.sciencemag.org/content/320/5873/190.full.html>

Supporting Online Material can be found at:

<http://www.sciencemag.org/content/suppl/2008/04/10/320.5873.190.DC1.html>

This article has been **cited by** 187 article(s) on the ISI Web of Science

This article has been **cited by** 2 articles hosted by HighWire Press; see:

<http://www.sciencemag.org/content/320/5873/190.full.html#related-urls>

This article appears in the following **subject collections**:

Physics, Applied

http://www.sciencemag.org/cgi/collection/app_physics

Magnetic Domain-Wall Racetrack Memory

Stuart S. P. Parkin,* Masamitsu Hayashi, Luc Thomas

Recent developments in the controlled movement of domain walls in magnetic nanowires by short pulses of spin-polarized current give promise of a nonvolatile memory device with the high performance and reliability of conventional solid-state memory but at the low cost of conventional magnetic disk drive storage. The racetrack memory described in this review comprises an array of magnetic nanowires arranged horizontally or vertically on a silicon chip. Individual spintronic reading and writing nanodevices are used to modify or read a train of ~ 10 to 100 domain walls, which store a series of data bits in each nanowire. This racetrack memory is an example of the move toward innately three-dimensional microelectronic devices.

There are two main means of storing digital information for computing applications: solid-state random access memories (RAMs) and magnetic hard disk drives (HDDs). Even though both classes of devices are evolving at a very rapid pace, the cost of storing a single data bit in an HDD remains approximately 100 times cheaper than in a solid-state RAM. Although the low cost of HDDs is very attractive, these devices are intrinsically slow, with typical access times of several milliseconds because of the large mass of the rotating disk. RAM, on the other hand can be very fast and highly reliable, as in static RAM and dynamic RAM technologies. The architecture of computing systems would be greatly simplified if there were a single memory storage device with the low cost of the HDD but the high performance and reliability of solid-state memory.

Racetrack Memory

Because both silicon-based microelectronic devices and HDDs are essentially two-dimensional (2D) arrays of transistors and magnetic bits, respectively, the conventional means of developing cheaper and faster devices relies on reducing the size of individual memory elements or data storage bits. An alternative approach is to consider constructing truly 3D devices. One such approach is “racetrack” memory (RM) (*1*), in which magnetic domains are used to store information in tall columns of magnetic material arranged perpendicularly on the surface of a silicon wafer (Fig. 1). Magnetic domain walls (DWs) (*2*) are formed at the boundaries between magnetic domains magnetized in opposite directions (up or down) along a racetrack (Fig. 2). Each domain has a head (positive or north pole) and a tail (negative or south pole). Successive DWs along

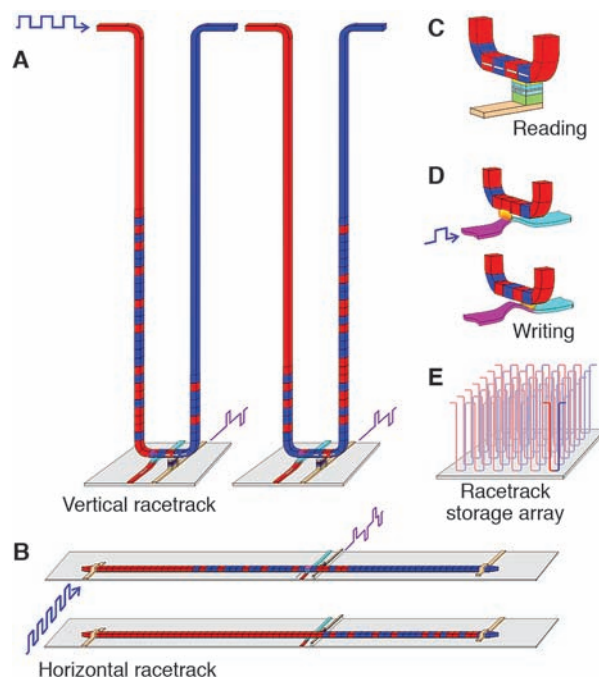


Fig. 1. The racetrack is a ferromagnetic nanowire, with data encoded as a pattern of magnetic domains along a portion of the wire. Pulses of highly spin-polarized current move the entire pattern of DWs coherently along the length of the wire past read and write elements. The nanowire is approximately twice as long as the stored DW pattern, so the DWs may be moved in either direction. **(A)** A vertical-configuration racetrack offers the highest storage density by storing the pattern in a U-shaped nanowire normal to the plane of the substrate. The two cartoons show the magnetic patterns in the racetrack before and after the DWs have moved down one branch of the U, past the read and write elements, and then up the other branch. **(B)** A horizontal configuration uses a nanowire parallel to the plane of the substrate. **(C)** Reading data from the stored pattern is done by measuring the tunnel magnetoresistance of a magnetic tunnel junction element connected to the racetrack. **(D)** Writing data is accomplished, for example, by the fringing fields of a DW moved in a second ferromagnetic nanowire oriented at right angles to the storage nanowire. **(E)** Arrays of racetracks are built on a chip to enable high-density storage.

the racetrack alternate between head-to-head and tail-to-tail configurations. The spacing between consecutive DWs (that is, the bit length) is controlled by pinning sites fabricated along the racetrack. There are several means of creating such pinning sites; for example, by patterning notches along the edges of the racetrack or modulating the racetrack’s size or material properties. Besides defining the bit length, pinning sites also give the DWs the stability to resist external perturbations, such as thermal fluctuations or stray magnetic fields from nearby racetracks.

RM is fundamentally a shift register in which the data bits (the DWs) are moved to and fro along any given racetrack to intersect with individual reading and writing elements integrated with each racetrack (Fig. 1). The DWs in the magnetic racetrack can be read with magnetic tunnel junction magnetoresistive sensing devices (*3*) arranged so that they are close to or in contact with the racetrack. Writing DWs can be carried out with a variety of schemes (*1*), including using the self-field of currents passed along neighboring metallic nanowires; using the spin-momentum transfer torque effect (*4, 5*) derived from current injected into the racetrack from magnetic nanoelements; or using the fringing fields from the controlled motion of a magnetic DW in a proximal nanowire writing element (*1*).

Uniform magnetic fields cannot be used to shift a series of DWs along the racetrack: Neighboring DWs would move in opposite directions and so eventually annihilate each other. Magnetic memory devices using non-uniform local magnetic fields to manipulate DWs were studied several decades ago (*6, 7*) but were abandoned because of their complexity and cost.

In RM, DWs are shifted along the racetrack by nanosecond current pulses using the phenomenon of spin-momentum transfer (*4, 5*). When a current is passed through a magnetic material, it becomes spin-polarized because of spin-dependent diffusive scattering, and so carries spin angular momentum (*3, 8*). When the spin-polarized current is passed through a DW, the current transfers spin angular momentum to the wall, thereby applying a torque to the moments in the DW, which can result in motion of the wall

IBM Almaden Research Center, San Jose, CA 95120–6099, USA.

*To whom correspondence should be addressed. E-mail: parkin@almaden.ibm.com

(9–15). The direction of motion of the DWs is independent of the magnetic charge of the DW, whether head to head or tail to tail, so that an entire sequence of DWs can be shifted along the racetrack. The magnetic columns need to be sufficiently narrow ($< \sim 100$ nm) for the spin momentum transfer interaction of the current with the DW to dominate over the self-field of the current. Thus, the racetracks are composed of nanowires of magnetic material approximately 100 nm or less in diameter and one to several tens of micrometers tall, thereby accommodating ~ 10 to 100 DWs per racetrack. The cost of storing one data bit in the RM is lowered as the number of DWs (n) that are stored in an individual racetrack increases, and, moreover, the average time needed to read a particular bit is independent of n if the distance between DWs is kept constant.

Fabricating the 3D RM is a substantial challenge (16). However, RM can also be built in a 2D geometry (Fig. 1B), which is much simpler. Moreover, even though a 2D RM has lower density than a 3D RM, its density is superior to that of nearly all other solid-state memories, including the densest flash memory (16) (table S1). The planar geometry is also more suitable for exploring the RM physics in a laboratory environment.

One of the most challenging aspects of RM is the controlled and reliable motion of a series of DWs, which are the data bits, backward and forward along the racetrack. The ultimate performance of RM will depend both on the current density required to move DWs and the velocity at which the DW pattern can be shifted along the racetrack. Thus, a detailed understanding of the magnetization dynamics of DWs and their interaction with spin-polarized current is key for the successful development of RM.

DW Data Bit

Current-driven DW motion has been studied in just a small number of magnetic materials, both “soft” and “hard” (17–30), in in-plane and perpendicularly magnetized nanowires, respectively. In hard materials, the magnetization direction is determined largely by the direction of the magnetic anisotropy fields, which are intrinsic to the material. In contrast, the magnetization direction in magnetically soft nanowires is defined by the geometrical shape and form of the nanowire. Here we focus on horizontal racetracks with rectangular cross-sections fabricated from thin films of soft magnetic alloys composed of iron, nickel, and cobalt. In these cases, the internal structure of the DW and its width are largely derived from magnetostatic fields determined by the shape of the racetrack (2). In particular, the DW width scales approximately with the nanowire width.

For the nanowire dimensions studied—widths ranging from 100 to 500 nm and thicknesses ranging from 10 to 50 nm—the DW states with the lowest energies have either transverse (T) or vortex (V) wall structures (31, 32) (Fig. 2, A and B). The vortex structure is favored in

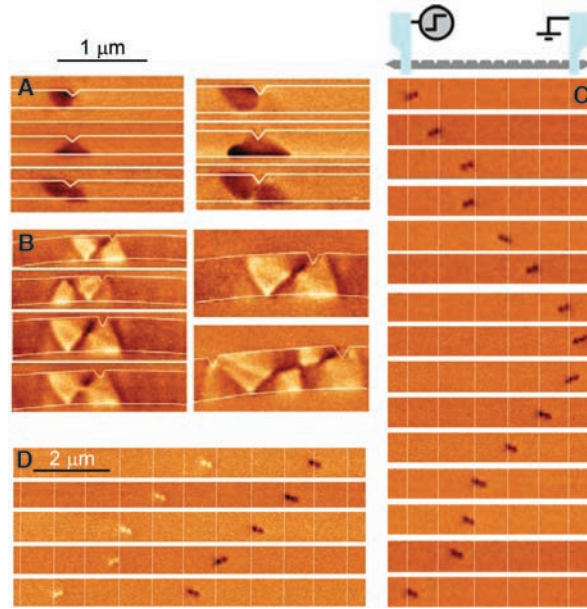


Fig. 2. MFM was used to probe the detailed structure of DWs pinned at a triangular notch in Py nanowires. The magnetic contrast (white or dark) depends on the charge of the DWs, whether head to head or tail to tail. Solid white lines show the nanowire’s topography as determined by atomic force microscopy. **(A)** Structure of tail-to-tail DWs observed in thin 10-nm-thick nanowires with widths of 200 nm (left) and 300 nm (right). From top to bottom, images show DWs with anticlockwise transverse, clockwise transverse, and anticlockwise vortex structures. **(B)** Structure of head-to-head DWs observed in 40-nm-thick nanowires with widths from 200 to 400 nm. The leftmost four images show examples of vortex DWs with clockwise and anticlockwise chiralities, both with negative core polarity (top two images on the left, for a nanowire width of 200 nm), and clockwise vortex walls with negative and positive core polarities (bottom two images on the left, width 300 nm). The two images on the right show examples of structures found in a 400-nm-wide nanowire: a vortex wall with clockwise chirality and negative polarity (top) and a more complex structure comprising two vortices and one antivortex for a DW pinned between two neighboring notches (bottom). **(C)** MFM was used to image the motion of a single tail-to-tail vortex DW. The cartoon at top shows a schematic of the experiment. A nanowire comprising a series of notches was connected to electrical contacts at each end to allow for injection of current pulses. Experimental results are shown for a 40-nm-thick, 100-nm-wide permalloy nanowire with 11 triangular notches located 1 μm apart; a part of the nanowire with six notches, indicated by vertical white dotted lines, is shown. Single current pulses, 8V (26 mA) and 14 ns long, were applied between each image sequentially from top to bottom. For the first eight images, pulses with negative polarities were applied. For the last seven images, pulses with positive polarities were applied. **(D)** The motion of two DWs in the same nanowire as in (C). Positive current pulses (26 mA, 14 ns long) were applied between successive images sequentially from top to bottom.

thicker or wider nanowires because it is flux closed with reduced surface charge (and, thereby, demagnetizing fields) at the nanowire edges. In larger nanowires, even more complex DW structures can be found (Fig. 2B). It is common to find both T and V DW structures in a given nanowire, for a wide range of nanowire widths and thicknesses, even when the DW energies are substantially different (Fig. 2A).

Even when only vortex DWs are energetically stable, several metastable vortex structures can be observed: The chirality of the vortex can be either clockwise or anticlockwise, and the vortex core polarity (that is, the direction of the out-of-plane vortex core magnetization) can be either negative or positive (Fig. 2B). Both the chirality and the polarity of the vortex strongly affect the DW dynamics. For example, the pinning strength of a notch depends on the DW chirality (33).

Current-Driven DW Motion

Perhaps the key concept underlying RM is the controlled movement of DWs along the racetrack by means of short pulses of spin-polarized current. This concept is demonstrated in Fig. 2C for permalloy (Py, $\text{Ni}_{81}\text{Fe}_{19}$) nanowires by measurement of the position, quasi-statically with magnetic force microscopy (MFM), of one or more DWs created in the nanowires. A sequence of MFM images was recorded after the injection of single current pulses or trains of pulses of varying length and magnitude along the nanowire. The DWs don’t move until a critical current threshold is exceeded. In Fig. 2C, the controlled motion of vortex DWs between successive notches is clearly shown for 14-ns-long pulses corresponding to a current density of $\sim 3 \times 10^8$ A/cm². Depending on the current direction, the DWs are moved in either direction along the nanowire, but the DWs’ motion is in the direction of the electron flow (that is, opposite to the current direction). Under these experimental conditions, the motion of the DWs is not reliable: In some cases, the DWs don’t move, move only across a

notch, or, on the contrary, skip a notch.

Under the same experimental conditions it is also possible to controllably move two DWs (Fig. 2D). The two DWs move in the same direction—with the electron flow—even though they have opposite magnetic charge. This demonstrates the feasibility of shifting a series of DWs with opposite charges along the racetrack. However, an important drawback of

these studies is that the threshold current density is so high that the nanowire temperature increases because of severe Joule heating from the current pulses. The heat capacity of the nanowire is so small that its equilibrium temperature is reached very quickly, within ~ 2 to 20 ns depending on the thermal link to the underlying substrate. In extreme cases, the nanowire's temperature can approach that of the Curie temperature of Py (~ 850 K). This obviously has deleterious results, including the possibility of the creation or annihilation of pairs of DWs. Reversals in the chirality (33) or polarity of the DWs and transformations of the DW structure (20) can also be seen at these high current densities, influenced not only by thermal perturbations but also by spin-momentum transfer itself. Thus, for the successful operation of RM, it is important to reduce the critical current density for moving DWs.

Critical Current for DW Motion

Understanding the origin of the critical current and its dependence on the racetrack's material and geometry has been a challenge for experimental and theoretical physicists in the past few years. Let us first compare DW motion driven by current and magnetic field. The field analog of the critical current density J_c is the propagation (or coercive) field H_p , below which no motion occurs. The origin of this propagation field is extrinsic: For an ideal racetrack, without any defects or roughness, DWs would move for any nonzero applied field, albeit very slowly. Thus, nonzero values of the propagation field are directly related to defects, which provide local pinning sites for the DW. In fact, H_p is proportional to the pinning strength, which can be tuned, for example, by fabricating notches with variable depths.

Intuitively, one would expect current-driven DW motion to follow the same behavior: The stronger the pinning, the larger the critical current. However, the original theories of spin-transfer torque suggested the existence of an intrinsic critical current density, even for an ideally smooth nanowire (11, 12, 14). In these theories, for currents smaller than this threshold value, DWs move only a short distance before stopping as they reach a dynamical equilibrium (for which the influx of spin angular momentum is compensated by damping). The critical current is independent of pinning strength (except for extremely strong pinning) and depends only on the racetrack's geometry and material parameters. More recently, it has been proposed that in addition to this original adiabatic spin-transfer torque term, there is another contribution that behaves as a magnetic field localized at the DW, which is often described as a nonadiabatic term. Even though the origin of this term is still under debate (13–15), its mere existence has dramatic effects on the current-driven DW dynamics. Indeed, the critical current becomes extrinsic; that is, it scales with the pinning strength. Thus, it follows that the critical current could be controlled by engineering pinning sites along the racetrack.

The relationship between critical current and pinning strength for vortex DWs is shown in Fig. 3A. These data suggest the existence of two different regimes. For relatively weak pinning (below ~ 15 Oe), the critical current density scales linearly with the pinning field. For the lowest pinning strength (~ 5 Oe), the critical current is on the order of 10^8 A/cm². For stronger pinning (>15 Oe), the critical current appears to saturate and becomes independent of pinning strength. In this regime, however, DW motion requires very high current densities resulting in significant Joule heating, and experimental data are thus difficult to interpret. These data suggest the existence of a nonadiabatic term in the spin-transfer torque. Indeed, the critical current in the low pinning regime seems to tend to zero for zero pinning, suggesting a purely extrinsic origin [a similar dependence was observed in multilayers with perpen-

dicular anisotropy (29)]. However, we cannot rule out the existence of a nonzero critical current for very low pinning (<5 Oe). Further work is needed to achieve such an extremely low pinning.

To date, the critical current to move a transverse DW in zero field has not yet been determined. It appears, as is consistent with theoretical models, that the threshold current for the motion of a transverse DW is higher than that for a vortex DW. It could be that in nanowires of appropriate dimensions (such as those with squarer cross-sections), transverse DWs can be moved.

DW Velocity

The maximum DW velocity that can be achieved is an important parameter that will ultimately determine the speed of RM. We have measured the DW velocity as a function of magnetic field and current density by using time-resolved resistance measurements (21, 24, 34).

Figure 3B shows the dependence of the DW velocity on magnetic field and current density. The DW velocity peaks at a relatively low magnetic field (~ 10 Oe), above which a negative DW mobility is observed (that is, the velocity decreases when the field increases). This drop in the DW velocity is associated with a change in the DW propagation mode and is known as the Walker breakdown (34–36).

Depending on the field, the DW moves with or without changing its structure. These different regimes are delineated by the Walker breakdown field. Above this field, as the DW moves, its structure transforms in a highly coherent manner, periodically switching between different states. This was observed recently as a periodic variation in the resistance of a moving DW (34). It was found that the oscillation period increased linearly with field but was little influenced by current, even though the DW's velocity was substantially changed. These results give direct evidence for the precessional nature of the DW's dynamics.

When spin-polarized currents are injected into the nanowire, the DW's velocity can be substantially modified (21, 22). The right panel of the inset in Fig. 3B shows that the field-driven DW's velocity varies linearly with current. Its velocity is increased or decreased here by up to 110 m/s when the electron flow is in the same or in the opposite direction to the pressure applied by the magnetic field. For magnetic fields smaller than

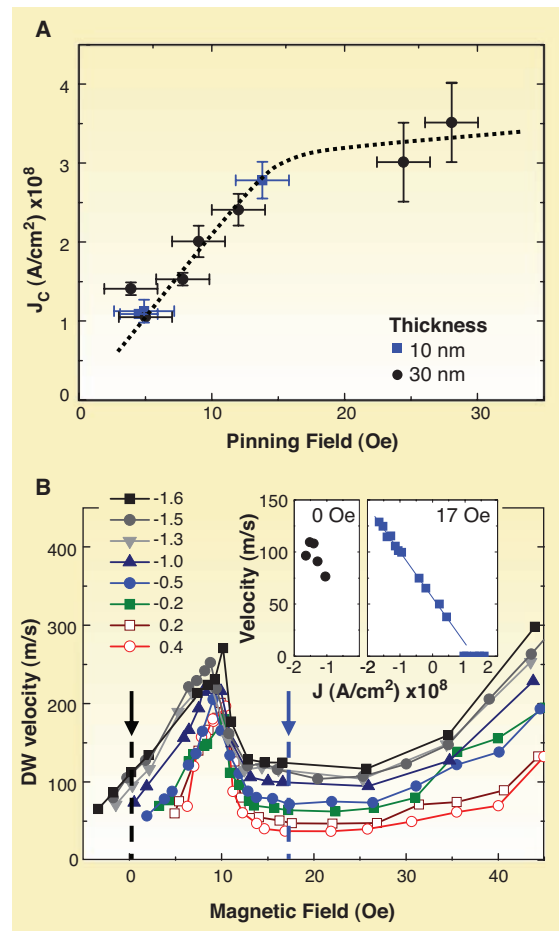


Fig. 3. (A) Critical current for depinning a vortex DW near zero field versus depinning field, measured on 10- and 30-nm-thick and 100- to 300-nm-wide Py nanowires using current pulses 20 to 100 ns long. The dotted line is a guide to the eye. (B) DW velocity plotted against magnetic field for various current densities flowing across the DW for Py nanowires 10 nm thick and 300 nm wide. Current densities indicated in the figure are in units of 10^8 A/cm². Solid and open symbols represent negative and positive currents, respectively. Negative current corresponds to electrons flowing along the field-driven motion of DWs. (Insets) DW velocity versus current density at fixed magnetic fields.

~ 5 Oe, field alone cannot drive the DW along the nanowire because of local random pinning from edge and surface roughnesses. However, current can move the DW even in the absence of any magnetic field. The left panel of the inset in Fig. 3B shows the dependence of the velocity on the current density near zero field. The velocity exhibits a maximum value of ~ 110 m/s at a current density of $\sim 1.5 \times 10^8$ A/cm² (24). Such velocities are high enough for the RM to operate at clock rates that are competitive with those of existing technologies (table S1).

Resonant Amplification of DW Motion

In order to build a RM with stable bits, the DWs are located at specially fabricated pinning sites, suitably spaced along the racetrack. This means, however, that the current densities needed to move the DWs between these sites might be too high for practical use, in particular for nanowires formed from a single layer of Py. A novel method for lowering the critical current density of pinned DWs was recently demonstrated, which involves using short current pulses with particular lengths, matched to the innate precessional frequency of the pinned DW (23, 26). It has long been realized that many properties of a DW can be described as if the DW has a mass (37); just like a mechanical oscillator, a DW confined in a potential well resonates at a natural frequency when subjected to an excitation. This means that the amplitude of the DW's oscillatory motion can be resonantly amplified by properly engineering the profile of the current excitation, thereby substantially reducing the critical current (Fig. 4).

Insight into the DW's response to current excitation is obtained from a 1D model of the DW dynamics (37). The model is based on the Landau-Lifshitz-Gilbert equation, which describes the magnetization dynamics, including the DW's interaction with current.

When a small current is applied, the DW's position within the potential well and its energy undergo damped oscillations, eventually reaching a stationary state but with an increased energy proportional to the current (Fig. 4A, c). When the current is turned off, the DW oscillates toward its original equilibrium position at the bottom of the pinning potential. The details of the DW's trajectories during and after current excitation are strongly influenced by the duration of the current excitation (Fig. 4A, d and e). When the current pulse length is matched to approximately a half integer of the DW's precessional period τ_p (such as $1/2$, $3/2$, $5/2$, etc.), the DW can have sufficient energy to be driven out of the pinning site; whereas for pulses just a half-integer period longer (or shorter), the DW's energy is lower and it remains confined. Thus, the probability of depinning a DW from a pinning site oscillates with the current pulse length, which is a direct manifestation of the current-induced precessional excitation of the DW.

Experimental observation of this effect is shown in Fig. 4A, a and b, for two nanowires

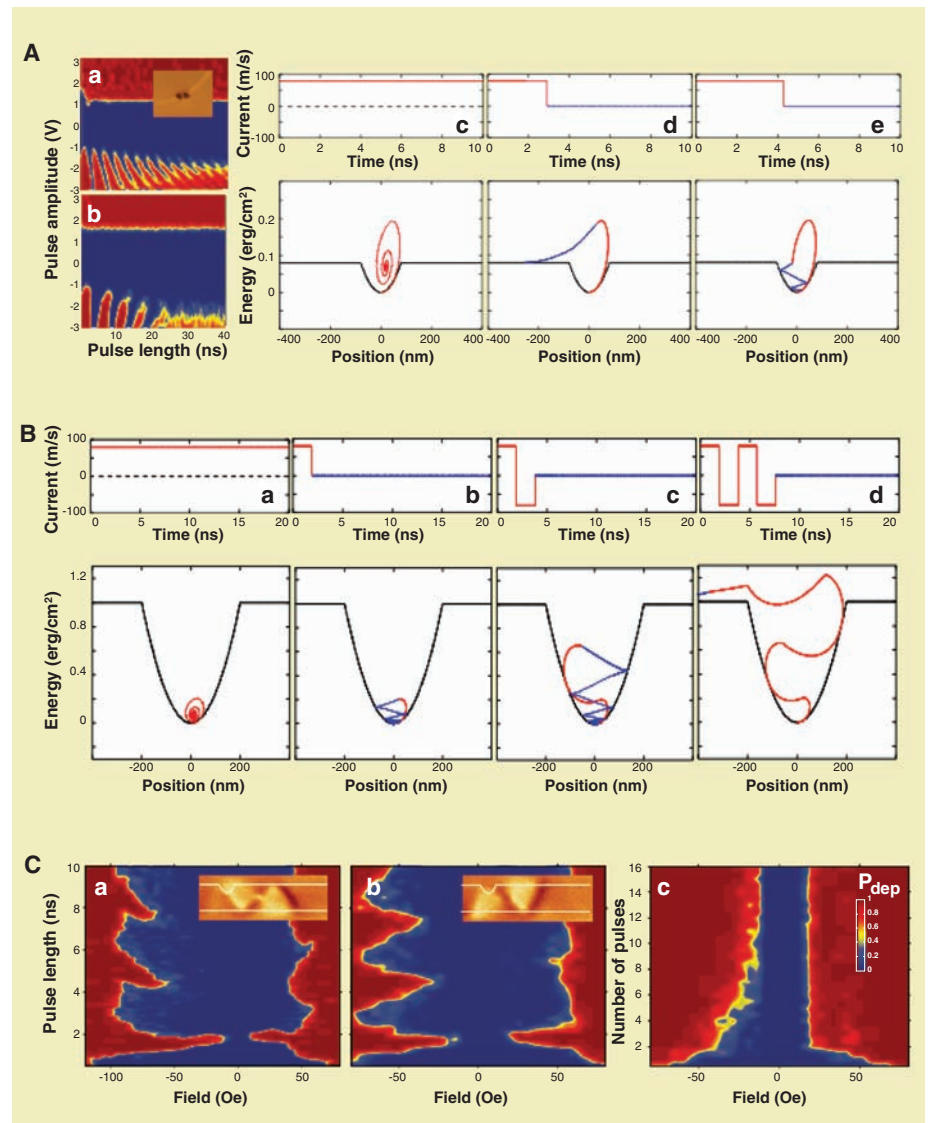


Fig. 4. Resonant amplification of DW motion can be used to reduce the current density required to move DWs from pinning sites. **(A)** Experimental observation of the DW oscillation confined in a potential well. **(a)** Probability of DW motion versus pulse length and amplitude, measured in an L-shaped nanowire (200 nm wide and 40 nm thick). The DW is weakly pinned at a local defect in the bend. A magnetic field of ~ 25 Oe was applied to assist DW motion. When the electron flow is along the field-driven motion direction (positive voltages), the DW is depinned only when the current density exceeds a threshold value, which does not depend on the pulse length. In contrast, when the electron flow opposes the DW motion direction, oscillations of the depinning probability are observed. **(b)** Probability map measured under the same conditions for a wire 100 nm wide and 40 nm thick. **(c to e)** Current-driven dynamics of a DW pinned in a shallow parabolic potential well, calculated with a 1D analytical model. The top panels show the current profile versus time for dc currents (c), a pulse at resonance [(d), pulse length 2.9 ns] and a pulse out of resonance [(e), pulse length 4.3 ns]. The bottom panels show the DW energy as a function of its position during (red) and after (blue) the current pulse. Also shown is the parabolic pinning potential well (black). **(B)** Analytical calculations of the dynamics of a DW pinned in a deep potential well. The DW trajectory in the energy/position space is plotted for dc current (a), a single pulse at resonance (length = 1.9 ns) (b), one bipolar pulse at resonance (c), and two bipolar pulses at resonance (d). **(C)** Experimental maps of the depinning probability for clockwise (a) and anticlockwise (b) head-to-head DWs pinned at the righthand side of a triangular notch in a nanowire 200 nm wide and 40 nm thick. The insets show the corresponding MFM images. The depinning probability is measured as a function of the external field and the pulse length for a series of 16 bipolar pulses, with an amplitude of 1 V. **(c)** Depinning probability (P_{dep}) map as a function of the applied field and the number of bipolar pulses applied at resonance (pulse length, 1.9 ns) for the anticlockwise DW shown in (b).

with different widths. The DW is pinned at a local defect in the curved region of the L-shaped nanowires. For negative voltages, the depinning probability oscillates with the current pulse length according to the mechanism described above (23), but with a longer period in the narrower wire because of the higher mass of the DW in the latter case. A magnetic field was applied to aid the DW's motion so that the oscillatory depinning effect was observed only for one current direction (here, negative).

When the pinning potential is deeper, a single current pulse with the same amplitude as in the previous example does not allow the DW to be depinned (Fig. 4B, b). However, just like a mechanical oscillator, the DW's energy can be resonantly enhanced by applying a series of current pulses synchronized with the oscillatory motion of the DW. This is illustrated in Fig. 4B, c and d, for the case of current pulses each exactly $1/2 \tau_p$ long, but with successive pulses of opposite polarities. The DW energy increases with each successive pulse until it is larger than the potential depth and the DW can be depinned. This takes places at much lower currents than is otherwise possible with dc current or a single current pulse (26).

Experimental evidence of the resonant amplification of DW motion is shown in Fig. 4C. Vortex DWs with either clockwise (a) or anticlockwise (b) chiralities are pinned at the righthand side of a triangular notch, which provides strong pinning. The probability of DW motion is shown as a function of the applied field and the pulse length, for a series of 16 bipolar pulses of fixed amplitude of 1 V ($\sim 10^8$ A/cm²). When the pulse length equals $1/2 \tau_p$ (~ 2 ns), the DWs are depinned with greater probability. Resonant amplification also occurs when the length of the pulse is increased by integer multiples of the resonance period but with progressively reduced efficiency. The shorter the current pulse, the more efficient is the phenomenon. Moreover, the phenomenon is only weakly dependent on the pinning potential [the resonance frequency depends on the square root of the slope of the potential well (23)] and on the DW's structure (for example, the chirality and polarity of vortex DWs). These attributes make the possibility of resonant DW depinning very useful for RM.

For the resonant amplification of DW motion to be useful in RM, it is important that depinning be achieved for a short series of pulses. Figure 4C, c shows experimental mapping of the depinning probability at resonance as a function of the applied field and the number of pulses for a series of bipolar pulses (1 V, 1.9 ns long) for the same DW as in Fig. 4C, b. Resonant amplification (in this case leading to the reduction of the depinning field) is substantial for just a single bipolar pulse and saturates for short trains of pulses (two to eight, depending on the depinning direction).

Outlook

There is much discussion about the possibility of developing 3D silicon microelectronic devices to

overcome the limitations of the further scaling of complementary metal oxide semiconductor transistors. These typically involve the thinning and stacking of several silicon chips in packages or the use of silicon through-wafer vias. RM is a 3D technology that is relatively simple in concept and potentially inexpensive to fabricate (16). By using the essentially unused space above the surface of a silicon wafer for storing data (in columns of magnetic material) and by "bringing" these data to the surface of the wafer for reading and manipulating the data, an intelligent 3D memory chip can be built with unsurpassed data storage capacities. Moreover, RM, by storing data as the direction of a magnetization vector, has no obvious fatigue or wearout mechanism, which plagues many nonvolatile memory technologies today that store information by physically moving atoms (such as phase-change or ferroelectric memory).

RM encompasses recent advances in the field of metal spintronics (3). Magnetoresistive devices based on the manipulation of the flow of spin-polarized current through metallic heterostructures composed of sandwiches of thin ferromagnetic electrodes separated by ultrathin metallic [typically copper (38)] or dielectric layers [the most useful being MgO (39)] have proven to be invaluable for sensing data bits in magnetic HDDs. Indeed, the first device—the spin valve—enabled a thousandfold increase in the storage capacity of such drives in the past decade (3). The second device—the magnetic tunnel junction (MTJ)—is in the process of supplanting the spin valve because of its higher signal. MTJs also form the basis of modern magnetic RAMs (MRAMs), in which the magnetic moment of one electrode is used to store a data bit. Whereas MRAM uses a single MTJ element to store and read one bit, and HDDs use a single MTJ to read all ~ 100 GB of data in a modern drive, RM uses one device to read ~ 10 to 100 bits. Depending on the number of DWs per racetrack and the velocity of the DW, the average access time of RM will be 10 to 50 ns, as compared to 5 ms for an HDD and perhaps ~ 10 ns for advanced MRAM.

RM uses spin-polarized current not only for sensing but also for manipulating magnetic information. Recent experiments establish its basic principles. DWs can be moved with nanosecond-long current pulses over distances of several micrometers and at high velocities exceeding 100 m/s (24). Moreover, DW motion using current alone enables moving a series of adjacent DWs (of alternating charge) in lockstep in one direction or the other by using current pulses of one sign or the other. However, there remain important challenges to overcome. Among these are the demonstration of the highly reliable motion of a series of ~ 10 to 100 DWs along the racetrack, and the reduction of the current density required for DW motion below the dc threshold values currently needed at room temperature, while maintaining high DW velocity. Further understanding of the interaction of spin-polarized current with mag-

netic moments is essential. Exploring a wide variety of materials and heterostructures may provide new insight into DW dynamics driven by current, making possible DW-based memory and possibly logic devices that were previously inconceivable.

References and Notes

- S. S. P. Parkin, U.S. Patents 6,834,005, 6,898,132, 6,920,062, 7,031,178, and 7,236,386 (2004 to 2007).
- A. Hubert, R. Schäfer, *Magnetic Domains: The Analysis of Magnetic Microstructures* (Springer, Berlin, 1998).
- S. S. P. Parkin *et al.*, *Proc. IEEE* **91**, 661 (2003).
- J. Slonczewski, *J. Magn. Magn. Mater.* **159**, L1 (1996).
- L. Berger, *Phys. Rev. B* **54**, 9353 (1996).
- R. E. Matick, *Computer Storage Systems and Technology* (Wiley, New York, 1977).
- S. Middelhoeck, P. K. George, P. Dekker, *Physics of Computer Memory Devices* (Academic Press, London, 1976).
- N. F. Mott, H. Jones, *Theory of the Properties of Metals and Alloys* (Oxford Univ. Press, Oxford, 1936).
- L. Berger, *Phys. Rev. B* **33**, 1572 (1986).
- L. Berger, *J. Appl. Phys.* **63**, 1663 (1988).
- G. Tataru, H. Kohno, *Phys. Rev. Lett.* **92**, 086601 (2004).
- Z. Li, S. Zhang, *Phys. Rev. Lett.* **92**, 207203 (2004).
- S. Zhang, Z. Li, *Phys. Rev. Lett.* **93**, 127204 (2004).
- A. Thiaville, Y. Nakatani, J. Miltat, Y. Suzuki, *Europhys. Lett.* **69**, 990 (2005).
- S. E. Barnes, S. Maekawa, *Phys. Rev. Lett.* **95**, 107204 (2005).
- See supporting material on Science Online.
- N. Vernier, D. A. Allwood, D. Atkinson, M. D. Cooke, R. P. Cowburn, *Europhys. Lett.* **65**, 526 (2004).
- A. Yamaguchi *et al.*, *Phys. Rev. Lett.* **92**, 077205 (2004).
- E. Saitoh, H. Miyajima, T. Yamaoka, G. Tataru, *Nature* **432**, 203 (2004).
- M. Kläui *et al.*, *Phys. Rev. Lett.* **94**, 106601 (2005).
- M. Hayashi *et al.*, *Phys. Rev. Lett.* **96**, 197207 (2006).
- G. S. D. Beach, C. Knutson, C. Nistor, M. Tsoi, J. L. Erskine, *Phys. Rev. Lett.* **97**, 057203 (2006).
- L. Thomas *et al.*, *Nature* **443**, 197 (2006).
- M. Hayashi *et al.*, *Phys. Rev. Lett.* **98**, 037204 (2007).
- S. Laribi *et al.*, *Appl. Phys. Lett.* **90**, 232505 (2007).
- L. Thomas *et al.*, *Science* **315**, 1553 (2007).
- M. Yamanouchi, D. Chiba, F. Matsukura, H. Ohno, *Nature* **428**, 539 (2004).
- D. Ravelosona, D. Lacour, J. A. Katine, B. D. Terris, C. Chappert, *Phys. Rev. Lett.* **95**, 117203 (2005).
- D. Ravelosona, S. Mangin, J. A. Katine, E. E. Fullerton, B. D. Terris, *Appl. Phys. Lett.* **90**, 072508 (2007).
- M. Feigenson, J. W. Reiner, L. Klein, *Phys. Rev. Lett.* **98**, 247204 (2007).
- Y. Nakatani, A. Thiaville, J. Miltat, *J. Magn. Magn. Mater.* **290–291**, 750 (2005).
- R. D. McMichael, M. J. Donahue, *IEEE Trans. Magn.* **33**, 4167 (1997).
- M. Hayashi *et al.*, *Phys. Rev. Lett.* **97**, 207205 (2006).
- M. Hayashi, L. Thomas, C. Rettner, R. Moriya, S. S. P. Parkin, *Nat. Phys.* **3**, 21 (2007).
- N. L. Schryer, L. R. Walker, *J. Appl. Phys.* **45**, 5406 (1974).
- G. S. D. Beach, C. Nistor, C. Knutson, M. Tsoi, J. L. Erskine, *Nat. Mater.* **4**, 741 (2005).
- A. P. Malozemoff, J. C. Slonczewski, *Magnetic Domain Walls in Bubble Material* (Academic Press, New York, 1979).
- S. S. P. Parkin, R. Bhadra, K. P. Roche, *Phys. Rev. Lett.* **66**, 2152 (1991).
- S. S. P. Parkin *et al.*, *Nat. Mater.* **3**, 862 (2004).
- We thank K. Roche and B. Gallagher for their contributions to this paper, R. Moriya and C. Rettner for help with sample preparation, and our colleagues in the Magnetolectronics group at Almaden for many useful discussions.

Supporting Online Material

www.sciencemag.org/cgi/content/full/320/5873/190/DC1
Materials and Methods
SOM Text
Tables S1 and S2
References

10.1126/science.1145799